Journal of Computational Science and Technology

Vol. 2, No. 1, 2008

Optimization of Blade Stiffened Composite Panel under Buckling and Strength Constraints*

Akira TODOROKI** and Masato SEKISHIRO***

**Department of Mechanical Sciences and Engineering, Tokyo Institute of Technology,
2-12-1 (i1-58), O-okayama, Meguro, Tokyo, Japan 152-8552
E-mail:atodorok@ginza.mes.titech.ac.jp

***Graduate student of Tokyo Institute of Technology
E-mail:msekishi@ginza.mes.titech.ac.jp

Abstract

This paper deals with multiple constraints for dimension and stacking-sequence optimization of a blade-stiffened composite panel. In a previous study, a multiple objective genetic algorithm using a Kriging response surface with a buckling load constraint was the target. The present study focuses on dimension and stacking-sequence optimization with both a buckling load constraint and a fracture constraint. Multiple constraints complicate the process of selecting sampling analyses to improve the Kriging response surface. The proposed method resolves this problem using the most-critical-constraint approach. The new approach is applied to a blade stiffened composite panel and the approach is shown to be efficient.

Key words: Optimization, Composites, Buckling, Fracture, Stacking Sequence, GA

1. Introduction

Composites are widely used for aerospace and automobile structures. Usually, laminated composites made by stacking unidirectional plies in multiple orientations are used for the structures because of the superior material properties of the laminated composites. It is crucial to optimize stacking sequences to take advantage of the laminated composites. Several researchers have proposed stacking sequence optimization methods [(1)-(8)]. In addition, a Fractal Branch and Bound (FBB) method optimizes the stacking sequence in a very short time [(9), (10)]. This method uses a quadratic polynomial to approximate the objective function such as the buckling load of a target structure, and then adopts lamination parameters as variables for the approximation of the response surface of the quadratic polynomial. Although the first FBB method was limited to an optimization of a single laminate, the method was modified to optimize multiple laminates such as panels and stiffeners [(11), (12)]. The FBB method has also been extended to a non-symmetrical laminate [(13)].

To minimize the structural weight, the dimensions of the composite structures including height and width of the stiffeners, spacing between the stiffeners and thickness, must be optimized with constraints such as buckling load and/or fracture load. To minimize the structural weight under certain constraints, the stacking sequences are also required to calculate the constraints such as buckling load. Authors have applied a Particle Swarm Optimization (PSO) method with a Kriging Response Surface (RS) and the FBB method to

*Received 4 Mar., 2008 (No. 08-0143)
[DOI: 10.1299/jcst.2.234]

minimize the weight of a hat-stiffened composite panel with a buckling load constraint [14]. The PSO method successfully optimizes a practical composite structure. It is, however, difficult to find a feasible result that satisfies a buckling load constraint with the progress of the optimization process in cyclic computations in PSO. A modified method that uses a Multi-Objective Genetic Algorithm (MOGA) with a Kriging RS and the FBB method has been successfully applied to the rocket interstage composite structure [15]. The MOGA method succeeds in obtaining the practical optimal result with low computational cost.

In the present study, the MOGA method with a Kriging RS is modified to optimize multiple constraints: buckling load and fracture load. Tsai-Wu's fracture rule is adopted here to calculate the safety factor of each ply, while the Kriging RS is used to obtain the approximated response of the constraints to reduce the computational cost. Improvements to the Kriging RS are performed at the end of each cycle of the MOGA by adding new sampling points. However, when two constraints are approximated using two Kriging RS's, the process of selecting new sampling points that can improve the fitness of the Kriging RS, is complicated. This paper deals with a single Kriging RS making the selection process simpler, which in turn means that the proposed method obtains the optimal practical result at lower cost. This method is applied to a weight minimization problem of a blade-stiffened composite panel.

2. Optimization problem

A composite panel with two blade-type stiffeners as shown in Fig. 1, is adopted as the target structure for optimization. The length of the panel is a=0.25m and the width is b=0.16 m. The width and length dimensions of the panel are fixed in the present study. The design variables of the blade-stiffened panel are the height of the blade (h), width of the flange (b_2), spacing from the edge to the blade (s), half number of plies of the panel (N_p) and the half number of plies of the stiffener (N_s). Both blades are placed symmetrically. The minimum and maximum limits of these design variables are listed in Table 1.

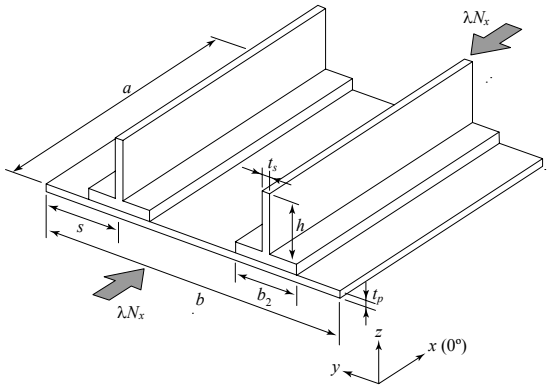

Fig.1 Blade-stiffened composite panel for optimization

Table.1 Design variables.

Design variable	Min.	Max.
h	0.01	0.05
b_2	0.02	0.04
s	0.03	0.05
N_p	4	16
N_s	4	16

The stiffened panel is subjected to the compression loading (N_x) as shown in Fig.1. The load is used as a reference load. The buckling load ratio (λ_b) is defined as a proportionality constant against this reference load when buckling occurs: $\lambda_b>1$ means the structure is safe from buckling. Fracture of each ply is judged by means of Tsai-Wu's fracture criterion, and the safety of each evaluation point is defined as a fracture factor (λ_s) against the reference load when the fracture occurs: $\lambda_s>1$ means the point is safe from fracture. In this study, the reference compression load is N_x=2.0MN/m. Under this load, both compression fracture as well as buckling is significant. Tsai-Wu's fracture criterion is given as:

$$F_{11}\sigma_1^2 + 2F_{12}\sigma_1\sigma_2 + F_{22}\sigma_2^2 + F_{66}\sigma_6^2 + F_1\sigma_1 + F_2\sigma_2 = 1 \quad (1)$$

where F_{11}, F_{12}, F_{22}, F_{66}, F_1 and F_2 are defined as follows.

$$F_{11} = \frac{1}{XX'}, F_{22} = \frac{1}{YY'}, F_{66} = \frac{1}{S^2}, F_1 = \frac{1}{X} - \frac{1}{X'}, F_2 = \frac{1}{Y} - \frac{1}{Y'}, F_{12} = F_{12}^*\sqrt{F_{12}F_{22}} \quad (2)$$

The material used here is T300/5208, all properties of the strength of which are shown in Table 2. For each stress element i (i=1,2,6), the fracture factor λ_s is defined as:

$$\sigma_i^{fracture} = \lambda_s \sigma_i^{applied} \quad (3)$$

where $\sigma^{fracture}$ denotes the stress that satisfies Tsai-Wu's criterion and $\sigma^{applied}$ the applied stress.

The fracture factor can be calculated for every integral point in each element. Since a first ply failure criterion is adopted in the present study, the minimum value of the fracture factor is adopted for the composite structure.

Table 2 Material properties of T300/5208

E_L	181GPa
E_T	10.3GPa
GLT	7.17GPa
ν_{LT}	0.28
ρ	1.6×10^3 kgf/m^3
X	1.5GPa
X'	1.5GPa
Y	40MPa
Y'	246MPa
S	68MPa
F'_{12}	-0.5

In the present study, ply thickness is t_{ply}=0.125mm. Since the panel and the stiffener are both symmetric laminates, the total thickness of the panel (t_p) and the stiffener (t_s) can easily be calculated as $t_p=2N_pt_{ply}$ and $t_s=2N_st_{ply}$. Total weight of the structure is calculated by means of the assumption of a thin-wall structure as follows:

$$W = \{bt_p + 2(b_2+h)t_s\}\rho a = \{bN_p + 2(b_2+h)N_s\}2\rho a t_{ply} \quad (4)$$

To analyze the buckling load and fracture of the composite structure, we use commercially available FEM code, ANSYS. For the FEM analyses, an eight-node linear laminated shell element (SHELL99) is adopted here. The precise number of nodes and elements is different for each analysis because of the difference in dimensions. A rough estimate of the total number of nodes is 3000, and of the total number of elements 10000.

Since a building block approach is usually adopted for the design of CFRP structures and with the lack of experimental data for various stacking sequences, the available fiber angles are limited to 0°, 90°, 45° and -45° in this study. Stacking sequences of the panel and stiffeners are symmetric, and the balance of the number of angle plies and the four-contiguous ply rule are adopted here; in other words, the same ply angle must not exceed four plies to prevent large matrix cracking.

The objective function of the optimization problem is to minimize the weight of the blade-stiffened composite panel under buckling load and fracture constraints. The problem

can be written as follows:

$$\text{Minimize } W \tag{5}$$

$$\text{subject to } \lambda_b \geq 1 \tag{6}$$

$$\lambda_s \geq 1 \tag{7}$$

3. Previous MOGA method with Kriging and FBB

3.1 Approximation with a Kriging RS

The objective function of the optimization problem is very simple, and it is easily calculated when all the dimensions of the blade-stiffened panel are fixed. The buckling load and fracture constraints, however, add a large computational cost because an FEM analysis is needed for each evaluation. In the present study, we use the objective function in Eq. (5) directly. On the other hand, the constraints of buckling load ratio (λ_b) and fracture factor (λ_s) are approximated using a Kriging RS to reduce the computational cost. The process of dealing with the multiple constraints is described later. All dimensions of the blade-stiffened panel and the lamination parameters of both panel and stiffener are used as variables for the response surface. Since the automatic process of constructing a Kriging RS is very useful, the DACE model is employed [14) - (16).

A Kriging RS based on the DACE model that comprises a response y and variable vector x_i (i=1,….,k) can be expressed as

$$\hat{y}(\mathbf{x}) = \mu + Z(\mathbf{x}) \tag{8}$$

where all variables are normalized between −1 and +1, for n sets of analyses, n sets of responses y_j (j=1,⋯,n) and variables x_{ij} (i=1,⋯,k and j=1,⋯,n). μ is a constant calculated as the average value of the global design space, and $Z(x)$ is the variable of the average value at the point x.

$Z(x)$ is expressed as a realization of a stochastic process of the normal distribution of the mean value of zero. A response value y at the point x is calculated as a correlation between the n sets of analytical results. The covariance matrix is given by

$$Cov\left[Z(\mathbf{x}^i), Z(\mathbf{x}^j)\right] = \sigma^2 \mathbf{R}\left[R(\mathbf{x}^i, \mathbf{x}^j)\right] \tag{9}$$

where **R** is the correlation matrix, and the element $R(x_i,x_j)$ is the value of a Gaussian correlation function between the points x_i and x_j. In the present study, the distance between two points of each variable may not be expressed on an identical scale. This means using scaled distances by multiplexing a constant to a distance, and the Gaussian correlation function can be written as

$$R(\mathbf{x}^i, \mathbf{x}^j) = \exp\left[-\sum_{m=1}^{k} \eta_m \left| x_m^i - x_m^j \right|^2\right] \tag{10}$$

where the η_m ($\eta_m \geq 0$, m=1,...,k) are unknown correlation parameters, which are required for the DACE model. In Eq. (10), x_m^i and x_m^j are the m^{th} elements of position vector x_i and x_j, respectively. The value of the correlation function is the degree of influence between two points against the response. A smaller value of η denotes influence from a greater distance; that is, the point is affected by the surrounding points. Since each design variable has a different scale for the correlation parameter, the strength of the effect of the correlation parameter can be controlled by means of the unknown value of η_m.

The expected response at a point x can be calculated as

$$\hat{y}(\mathbf{x}) = \hat{\mu} + \mathbf{r}^T \mathbf{R}^{-1}(\mathbf{y} - \mathbf{1}\hat{\mu}) \tag{11}$$

where $\hat{\mu}$ is an estimator of μ, **y** is a column vector that has n elements of response at the n sample points, **1** is a column vector whose elements are all 1 ($[1,...,1]^T$), and **r** is a column vector that has values of the correlation function between the target point and the other sample points.

$$\mathbf{r}(\mathbf{x}) = \left[R(\mathbf{x}, \mathbf{x}^1), R(\mathbf{x}, \mathbf{x}^2), \cdots, R(\mathbf{x}, \mathbf{x}^n)\right]^T \tag{12}$$

Assume that the values of **η**, a parameter of the DACE mode, are given, then $\hat{\mu}$ and

the variance of $\hat{\mu}$ ($\hat{\sigma}^2$) can be calculated as

$$\hat{\mu} = \frac{\mathbf{1}^T \mathbf{R}^{-1} \mathbf{y}}{\mathbf{1}^T \mathbf{R}^{-1} \mathbf{1}} \tag{13}$$

$$\hat{\sigma}^2 = \frac{(\mathbf{y} - \mathbf{1}\hat{\mu})^T \mathbf{R}^{-1} (\mathbf{y} - \mathbf{1}\hat{\mu})}{n} \tag{14}$$

The only remaining problem is how to obtain the parameter $\boldsymbol{\eta}$. To estimate the values of $\boldsymbol{\eta}$, we adopt a log likelihood function.

$$Ln(\boldsymbol{\eta}) = -[n \ln(\hat{\sigma}^2) + \ln|\mathbf{R}|]/2 \tag{15}$$

where $\hat{\sigma}^2$ and $\mathbf{R}$ are functions only of $\boldsymbol{\eta}$. The correlation parameter for $\boldsymbol{\eta}$ is obtained by maximizing the log likelihood function. In this problem, the number of unknown values is k. In the present study, the Particle Swarm Optimization method [14] is used to maximize the log likelihood function with the initial values proposed by Welch et al. [17]. After obtaining the correlation parameter $\boldsymbol{\eta}$, the estimator of Eq. (11) can be calculated and the variance of the estimator obtained from

$$s^2(\mathbf{x}) = \hat{\sigma}^2 \left[1 - \mathbf{r}^T \mathbf{R}^{-1} \mathbf{r} + \frac{(1 - \mathbf{1}^T \mathbf{R}^{-1} \mathbf{r})^2}{\mathbf{1}^T \mathbf{R}^{-1} \mathbf{1}} \right] \tag{16}$$

The estimator of the standard deviation is calculated as $s = \sqrt{s^2(\mathbf{x})}$, and the value is defined as an estimation error. The DACE model definitely passes all sampling points. The estimation errors at the sampling points are therefore, clearly zero, and the estimation error increases when the estimation point is located far from the adjacent sampling points.

When the estimation error is subjected to a normal distribution of $N(y,s^2)$, the probability that the response $y = f(x)$ exceeds a value of 1 is calculated as

$$\Pr(f(x) \geq 1) = \Phi\left(\frac{f(x) - 1}{s} \right) \tag{17}$$

where $\Phi(\ )$ is the cumulative distribution function, $f(x)$ is a response y of the Kriging (DACE) model at position x and s is the estimator of the standard deviation obtained from Eq. (16).

3.2 Design of Experiment

We have adopted Latin Hypercube Sampling (LHS) experiments [17], as LHS gives uniformly distributed sampling over the entire design space. The sample size required by the DACE model [18] is usually 10 times greater than the number of variables.

LHS is, however, not simple for composite structures, because lamination parameters are not independent variables. To solve this problem, all feasible symmetric laminates of 16 plies (with a half ply being eight) were prepared. The total number of feasible plies that satisfy the balanced rule of angle plies is 3281. From this set of feasible laminates, a set of n_s laminates is selected randomly with the constraints described below.

For the laminates of 16 plies, 25 sets of in-plane lamination parameters are feasible. As discussed before, the available fiber angles are limited to 0°, 45°, -45° and 90°. For the feasible laminates comprising these fiber angles, lamination parameters exist inside and on the boundary of the triangle (1,1), (-1,1), (0,-1). To obtain an equal distribution of the sampling for the in-plane lamination parameters, the three apices of the triangle are definitely selected at least once and another 22 points are selected at least twice. The selected laminates are feasible even when the total number of plies is changed by changing the ply thickness.

To select candidate points as variables of the dimensions, all variables are divided into n_s segments. For variables of the dimensions of structural components such as a blade-stiffener configuration, feasible design scopes of the variable are normalized between -1 and +1, and equal segmentations are adopted here. For the number of plies N, the numbers must be positive integers, which is achieved by rounding. From these segmented variables, a table is constructed of all segments and equally distributed sampling points are

obtained.

After obtaining the sampling points, an FEM analysis is performed at each sampling point. Using the FEM analyses results, a Kriging model of the buckling load ratio is constructed. We use n_s=251 in this research.

3.3 MOGA with Kriging and FBB

The algorithm for MOGA has already been published in a well-known textbook [19]. Since the MOGA process is similar to that of the simple GA, a detailed explanation is omitted. There are however, two points that differ from the simple GA: there are multiple objective functions which are not transformed into a single objective function, and the population of the MOGA is scattered over a wide range to obtain non-dominated solutions (Pareto solutions) distributed over the entire design region (the population must be rich in diversity). These differences are clearly defined in a reference [19]. The diversity of population is attained by means of the fitness shearing method [19].

In the present study, the structural weight of the blade-stiffened panel and the probability of satisfaction of the constraints are the target objectives of the MOGA. The structural weight is simply transformed into the reduction in weight from the provisional optimal result that is obtained in the previous computation. This transforms the problem into a maximization of the multiple objectives, namely the reduction in weight from the provisional optimal and the probability of satisfaction of the constraints. Recalling that the constraints are approximated here and that the Kriging RS is a simple approximated value, the probability of satisfaction is used rather than the direct response of the Kriging RS.

The present study employs a two-layer optimization process. In the upper layer, optimization of structural dimensions is performed by means of the MOGA. Chromosomes of each individual correspond to structural dimensions such as height or width of the stiffener, and these dimensions offer sufficient information to evaluate the structural weight. To evaluate the buckling load and fracture of the structure, however, stacking sequences of composite laminates must be known. The upper layer optimization process activates a lower layer optimization of the stacking sequences for this process. The stacking sequences of the stiffener and panel are optimized by the modified FBB method; this is a modified version of the FBB method to optimize more than two laminates simultaneously.

The flow of this optimization process is shown in Fig. 2 and can be summarized as follows .

(1) First, the design of experiments is performed using LHS to select n_s points. FEM analyses of buckling load are conducted at the selected n_s points. The Kriging RS is produced from the results of the n_s points. The value of n_s should be more than 10 times the number of design variables. From the n_s selected points, the minimum weight structure satisfying the buckling load constraint is selected as the provisional optimal structure (W_{min}).

(2) Initial individuals of the MOGA (total size of population is 100) are selected randomly.

(3) Upper layer optimization is performed using the MOGA.

(a) The fitness of each individual is evaluated; lower layer optimization is performed to optimize stacking sequences of the stiffener and panel using the extended FBB method to maximize the probability of the satisfaction of the constraint factor. This process is described later.

(b) Non-dominated individuals are searched for using the two objective functions, weight reduction from the provisional structure and the probability of satisfaction of the constraint factor.

(c) The diversity of population is evaluated for each individual, and the fitness value of each individual is calculated.

(d) Selection is performed using a Pareto ranking method, and a mutation is conducted after a crossover of the selected individuals.

(4) The MOGA is terminated at the 300th generation.

(5) The top ten individuals of the probability of satisfaction of the buckling load are calculated by means of FEM analyses while considering the diversity of the population in the 100 Pareto solutions.

The ten new FEM results are added to the Kriging RS data set. The process is then repeated from step (2).

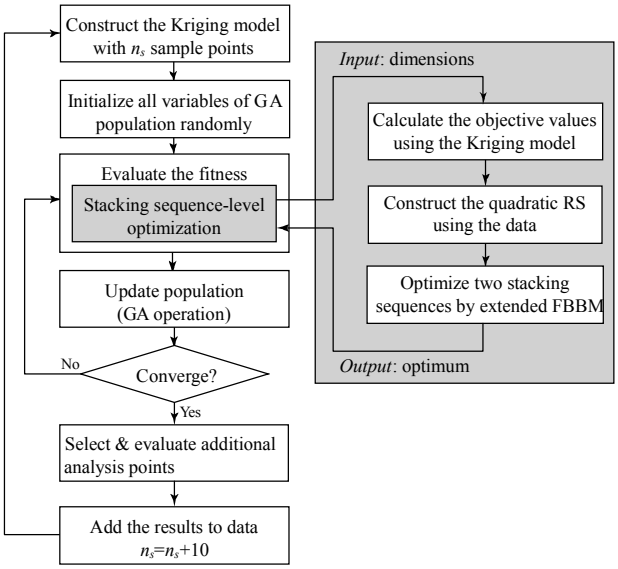

Fig. 2 Flowchart of multi-objective dimensions and stacking sequence optimization.

4. Improvement of the MOGA with Kriging and FBB

The previously mentioned MOGA method with a Kriging RS and FBB has been adopted in the optimization of composite interstage structures [15]. In the previous study, the only constraint was the buckling load ratio, whereas in this study there are two constraints: the buckling load ratio and the fracture factor. Both constraints must be greater than 1. The simplest method to deal with the multiple constraints is to make a Kriging RS for each constraint. This method, however, requires complicated procedures to select candidates to improve the approximation of the Kriging RS, and also adds computational cost in calculating the Kriging RS when the number of constraints is increased. Moreover, the increase in the objective functions of the MOGA makes obtaining the optimal Pareto results for the MOGA difficult.

In the present study, therefore, a modified approach is adopted. Only a single Kriging RS is used to approximate the most critical constraint. The definition of the most critical constraint λ_{min} is given by:

$$\lambda_{\min} = \min[\lambda_b, \lambda_s] \tag{18}$$

When $\lambda_{min}>1$, both λ_b and λ_s are larger than 1. This modification simplifies the optimization process of the MOGA, but may result in a non-smooth response surface for the constraint. The drawback is compensated by the fitness improvement process: with the selected candidates from the structures located close by, the probability of satisfaction of the constraint is equal to 1. This means the fitness of the Kriging RS is improved near the structures that satisfy both the constraints as the optimization progresses.

For the stacking sequence optimization, the probability of satisfaction of the most critical constraint λ_{min} is maximized using the FBB method. Since the probability of satisfaction shows rapid change around the sampling points, the variable $\{(\lambda_{min}-1)/s\}$ of Eq.

(17) is used as an objective function in the FBB method. At the sampling point, a smaller value of s is used instead of s=0. First, the design of the experiment is performed for the lamination parameters [9],[10],[11], and the value of λ_{min} and the variance of the estimation are obtained from the Kriging RS at each selected laminate. A quadratic polynomial response surface is constructed from the values of $\{(\lambda_{min}-1)/s\}$ using the least squares error method. The FBB simply searches the laminate that maximizes the probability of satisfaction of $\lambda_{min}>1$ because the cumulative distribution function of Eq. (17) is a simple monotonically increasing function.

To terminate the MOGA, the maximum number of MOGA cycles is set to 10 in the present study.

5. Results and discussion

Using LHS, the experiment was performed and 251 sampling points were selected. After concluding the FEM analyses at each sampling point, the first Kriging model was constructed using the FEM results. Figure 3 shows the cross validation estimation results of the first Kriging model. Since the cross validation process is usually to estimate a response of the sampling point after eliminating the target sampling point, the evaluated responses show the responses of the new data using the Kriging model. The abscissa is the actual value of λ_{min} and the ordinate the estimated values thereof. Figure 3 shows that the first Kriging RS has good estimations over the entire region.

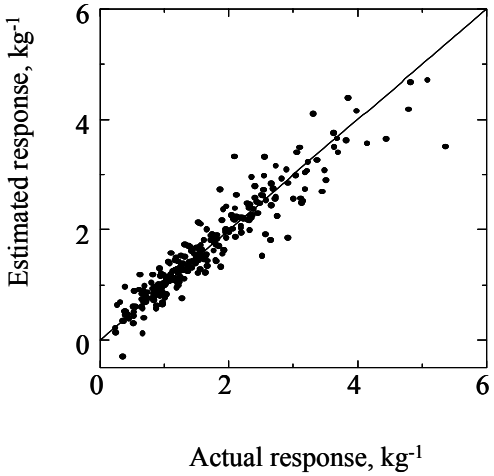

Fig. 3 Results of cross-validation of initial Kriging response surface.

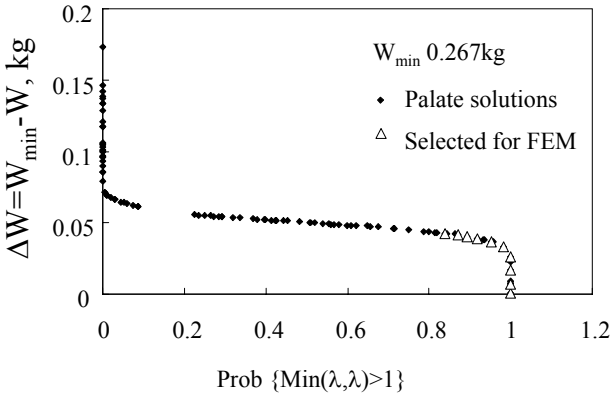

Fig. 4 Optimal Pareto solutions of the first MOGA cycle.

Figure 4 shows the provisional Pareto optimal results after the first cycle of the MOGA. The ordinate is the weight reduction and the abscissa the probability of satisfaction of λ_{min}. The plots are the results obtained after the first MOGA cycle, and the open triangle symbols are the selected individuals for the FEM analyses to improve the Kriging RS. Since the

constraint must be satisfied, the individuals with a higher probability of satisfaction of the constraint are selected to improve the Kriging RS near the optimal point. W_{min} represents the minimum weight of the initial 251 FEM analyses. The weight of each individual of the MOGA can be easily calculated from Eq. (4). This means that the ordinate is the exact value in Fig. 4.

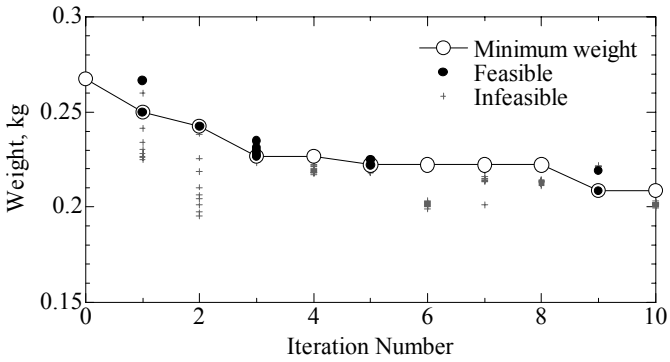

Fig. 5 Iteration history of the minimum weight of the MOGA.

Figure 5 shows the results of the history of the minimum weight of the MOGA. The abscissa is the iteration cycle number of the MOGA, and the ordinate the weight of the optimal Pareto results at each iteration cycle. The large open circles represent the minimum weight structures that satisfy the constraint, whereas the large solid circles represent the structures that satisfy the constraint but which are not the minimum weight structures. The cross-shape symbols represent the structures that do not satisfy the constraint. Figure 5 shows that it is difficult to obtain a better result with more optimization cycles.

Table 3 Optimal result.

W, kg	0.209
λ_b	1.05
λ_s	1.51
h	0.0119
b_2	0.0362
s	0.0361
N_p	4
N_s	15
Panel	$[45/\text{-}45/90_2]_S$
Stiffener	$[0_4/45/0_4/\text{-}45/0_4/90]_S$

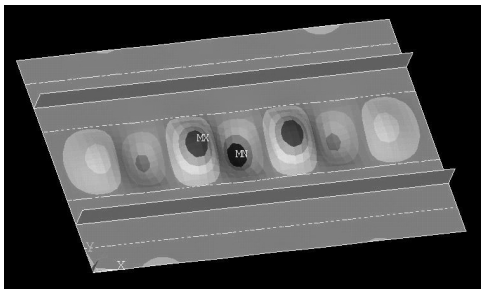

Fig. 6 Buckling mode of the optimal structure

Table 3 shows the optimal result obtained after the 10th iteration of the MOGA. The total number of FEM analyses is 251+100=351. Since the MOGA requires tens of thousands of FEM analyses without the Kriging model, the present MOGA with Kriging method is a very effective method of reducing the computational cost. For comparison, a dimension optimization was performed using material properties of a quasi-isotropic laminate. The weight of the optimal result using the quasi-isotropic laminate was 0.270kg. This means that the present optimization of dimensions and stacking sequences enables us

to obtain a 23 % lighter weight structure. Since the fracture point is at the point under the blade stiffener, the thick blade stiffeners seem to prevent fracture due to compression load. The buckling mode is illustrated in Fig. 6, where the panel part shows buckling first due to the thick blade stiffeners.

To investigate the modification of the DACE Kriging RS by adding extra FEM analyses, a cross validation of the 10th Kriging RS is performed as shown in Fig.7. The abscissa is the actual λ_{min} and the ordinate the estimated λ_{min}. Compared with the initial Kriging RS of Fig. 3, an extra 100 FEM analytical results are added to the data to make the Kriging RS in Fig. 7. The solid symbols represent the initial 251 data samples, while the open symbols are the extra 100 FEM analytical results added later. As shown in Fig.7, almost all the initial points give poor estimates for the average value and the Kriging RS gives good estimates only for the added new sampling data. This means that adding extra FEM data clearly improves the fitness around the optimal point, but makes the fitness of other areas worse.

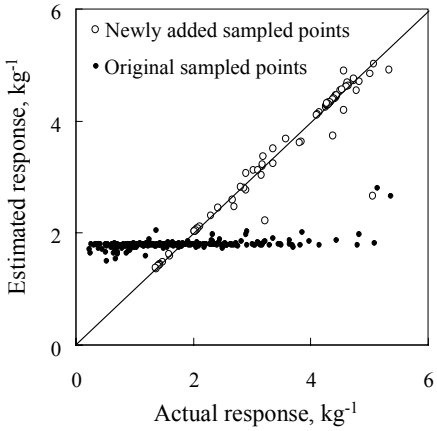

Fig. 7 Result of cross-validation of the 10th renewed Kriging model

Figure 8 represents the schema of the worsening mechanism for the initial sampling points of the DACE Kriging RS. The abscissa is a variable and the ordinate the response. The solid circle symbols are the initial sampling points and the open circle symbols the newly added points. The dash-dotted curve represents the initial response surface and the solid curve represents the renewed Kriging estimation curve.

With the increase in MOGA cycles, the number of added FEM analyses increases. This means many points around the optimal result are added to the Kriging RS. With the increase of concentrated sampling around the optimal points (x=0.62), the curve gives better estimates around the optimal point. The estimates far from the optimal point, however, are worse.

This concentrated sampling around the optimal result causes an increase in the Kriging correlation parameters η decided in Eq. (15). The increase in η means that the sampling points just near the target point affect the response. This, therefore, causes poor estimation for the area located far from the concentrated sampling point: the response far from the concentrated sampling point becomes the average value except for the points near the sampling points. Table 4 shows the correlation parameters for the first and 10th Kriging RS. As shown in Table 4, the correlation parameter values increase for many of the parameters.

Table 4 Comparison of correlation parameters of two Kriging RS

	V_{1p}^*	V_{2p}^*	W_{1p}^*	W_{2p}^*	V_{1s}^*	V_{2s}^*	W_{1s}^*	W_{2s}^*	h	b_2	s	N_p	N_s
1	0.567	0.587	0.016	0.031	0.425	0.037	0.036	0.067	0.914	0.048	0.160	0.520	0.415
10	1.994	1.777	9.538	1.108	9.295	0.017	0.000	0.001	72.64	7.357	0.978	13.13	1.200

When the estimation of the DACE Kriging RS is used directly, this worsening of fitting in the sparse sampling area definitely results in a fatal error for the optimization process. In the present study, however, the probability of satisfaction of the constraint is used for the optimizations of the stacking sequences. In the calculation of the probability, not only the response but also the variance (s) in Eq. (16) is used. The variance increases with the increase in distance from the sampling point. In this study, the poor fitness of the response does not affect the optimizations of the stacking sequences directly. This problem of exceedingly concentrated sampling must be checked when the response of the Kriging is used directly in the optimization process. Moreover, it is clearly not true that the addition of sampling points does not affect the fitting of response values in the data sparse region for the DACE Kriging RS. Even with the DACE Kriging RS, we have to be as careful as when using a polynomial response surface if we use the response value directly in the optimization process. Resolving this problem is our future work.

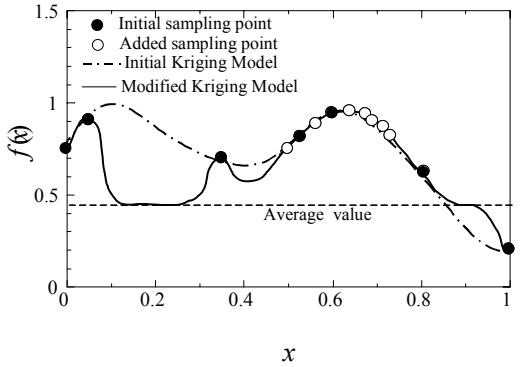

Fig. 8 Typical DACE Kriging RS with concentrated sampling

6. Concluding remarks

The present study deals with the simultaneous optimization of dimensions and stacking sequences using the MOGA with multiple constraints. The new method is applied to a blade-stiffened composite panel. The most critical constraint is selected at each sampling point and the Kriging RS is made to estimate the probability of satisfaction of the constraints. This method successfully obtained the optimal practical result with only a small number of FEM analyses. Although the addition of sampling around the optimal point provides better fitness around the optimal point, the concentrated sampling results in poor estimations for the points far from the optimal point. The present method is not affected by this poor fitness because the probability of satisfaction of the constraint is used for the objective function in the stacking sequence optimization. This check of the fitness reveals that the concentrated sampling may give poor fitness in the relatively sparse sampling areas even for a Kriging RS constructed using the DACE model.

References

(1) M. Miki, Design of Laminated Fibrous Composite Plates with Required Flexural Stiffness, ASTM STP, 864, pp.387-400(1985).

(2) H. Fukunaga, and T.W. Chou, Simplified Design Techniques for Laminated Cylindrical Pressure Vessels under Stiffness and Strength Constraints, J. of Composite Materials, Vol.22, No.10, pp.1156-1169(1988).

(3) R. Le Riche and R. T. Haftka, Optimization of Laminate Stacking Sequence for Buckling Load Maximization by Genetic Algorithm, AIAA J., Vol.31, No.5, pp.951-956 (1993).

(4) J.L Marcelin and P. Trompette, Optimal Structural Damping of Skis using a Genetic Algorithm, Structural Optimization, Vol.10, pp.67-70 (1995).

(5) N. Kogiso, L.T. Watson, Z. Gürdal, and R.T. Haftka, Genetic Algorithms with local

Improvement for Composite Laminate Design, Structural and Multidisciplinary Optimization, Vol.7, No.4, pp.207-218 (1994).

(6) M. Zako, N. Takano, and N. Takeda, Cost Effective Design Procedure for Laminated Composite Structure Based on GA, Science and Engineering of Composite Materials, Vol.6, No.2, pp.131-140(1997).

(7) M.H. Cho and S.Y. Rhee, Layup Optimization Considering Free-Edge Strength and Bounded Uncertainty of Material Properties, AIAA J., Vol. 41, No.11, pp.2274-2282 (2003).

(8) Y. Narita, Layerwise optimization for the maximum fundamental frequency of laminated composite plates, Journal of Sound and Vibration, Vol.263, No.5, 1005-1016 (2003).

(9) Y. Terada, A. Todoroki and Y. Shimamura, Stacking Sequence Optimizations Using Fractal Branch and Bound Method for Laminated Composites, JSME International J., Series A, Vol.44, No.4, pp.490-498 (2001).

(10) A. Todoroki and Y. Terada, Improved Fractal Branch and Bound Method for Stacking Sequence Optimizations of Laminated Composite Stiffener, AIAA J, Vol.42, No.1, pp.141-148 (2004).

(11) Masato Sekishiro and Akira Todoroki, Extended Fractal Branch and Bound Method for Optimization of Multiple Stacking Sequences of Stiffened Composite Panel, Advanced Composite Materials, Vol.15, No.3, pp.341-356 (2006).

(12) Akira Todoroki and Masato Sekishiro New Iteration fractal branch and bound method for stacking sequence optimizations of multiple laminates, Composite Structures, Vol.81, No.3, pp.419-426 (2007).

(13) Ryosuke Matsuzaki and Akira Todoroki, Stacking Sequence Optimization Using Fractal Branch and Bound Method for Unsymmetrical Laminates, Composite Structures, 78(4), 537-550 (2007).

(14) Akira Todoroki and Masato Sekishiro, Two-Level Optimization of Dimensions and Stacking Sequences for Hat-Stiffened Composite Panel, Journal of Computational Science and Technology, JSME, Vol.1, No.1, pp. 22-33 (2007).

(15) Masato Sekishiro and Akira Todoroki, Dimension and stacking sequence optimizations of large composite structures using Kriging and MOGA method, Journal of the Society of Materials Science Japan, Vol.56, No.5, pp. 432-437 (2007), (in Japanese).

(16) J.D. Martin and T.W. Simpson, Use of Kriging Models to Approximate Deterministic Computer Models, AIAA J., Vol.43, No.4, pp. 853-863 (2005).

(17) W.J. Welch, R.J. Buck, J. Sacks, H.P. Wynn, T.J. Mitchell, and M.D. Morris, Screening, Predicting, and Computer Experiments, Technometrics, Vol.34, No.1, pp. 15-25 (1992).

(18) D.R. Jones, M. Schonau and W.J. Welch, Efficient Global Optimization of Expensive Black-Box Functions, J. of Global Optimization, Vol. 13, No.4, pp.455-492 (1998).

(19) K. Deb, Multi-Objective Optimization Using Evolutionary Algorithms, John Wiley & Sons, Chichester (2001).